Volume 1 | Number 1 | Jan 2013 | Pages 1–100

Journal of
Materials Chemistry C

Materials for optical and electronic devices
www.rsc.org/materialsC

ROYAL SOCIETY
OF CHEMISTRY

ROYAL SOCIETY
OF CHEMISTRY

www.rsc.org/materialsC

Journal of Materials Chemistry C

Dynamic Article Links▶

ARTICLE TYPE

Journal of Materials Chemistry C Accepted Manuscript

Synthesis and studies of magnetic properties of high temperature stable Ni nanoparticles in nearly amorphous AlPO$_4$ matrix in oxidative atmosphere

Rajalaxmi Maharana,[a,b] M. Manivel Raja,[a] V.V. Bhanu Prasad,[a] Pradip Paik,[b] Subir Roy[a*]

5

Graphitized carbon coated Ni nano particles were synthesized in the AlPO$_4$ matrix in situ in oxidative atmosphere without using any foreign reducing agent. The Ni nano particles were evenly distributed in inactive AlPO$_4$ matrix and protected from the oxidation in air 10 up to 900°C. Carbon coating over the nano particles remained intact even when the samples were calcined at 900° C in air. Magnetizations of the Ni nano particles in the composite were approached to ~89% of their bulk magnetization value when calcined at 900°C in air. Magnetization increased with increasing the calcinations temperature up to 900° C.

INTRODUCTION

15 Nanocomposites comprising of soft magnetic nano particles and insulating matrices have recently been the subject of intensive research due to their multiple advantages which include reduced hysteresis losses at high frequencies, isotropy in magnetic properties, better corrosion resistant of the core magnetic 20 materials, stable magnetic properties at variable high frequencies, reduced interactions between the closely spaced magnetic particles and reduced agglomerations [1-2]. These nanocomposites find wide range of potential applications in nanoelectronic devices, e.g. magnetic recording media, drug 25 delivery, diagnostic medical tools such as magnetic resonance tomography, magnetic resonance imaging, catalysis etc. [3-7]. Apart from these, the magnetic nanocomposites possess unusual properties such as giant magneto resistive effect [8] and hence have potential applications for fabrication of super high density 30 data storage devices [5, 6]. Various synthesis techniques like sputtering [9], high energy ball milling [10], ion exchange [11], and sol-gel [12-13] have been used to embed nano magnetic particles in an inert, nonmagnetic matrix i.e. SiO$_2$, Al$_2$O$_3$ etc.. Each of these methods have their own limitations. It is reported 35 that magnetic nanocomposites based on SiO$_2$ matrix suffer from the drawbacks of higher inherent porosity due to network structure of the SiO$_2$ matrix and hence the magnetic component is very prone to surface oxidation to larger extent even at higher level of vacuum and inert atmosphere. Metal nanoclusters–Al$_2$O$_3$ 40 composites need to be consolidated above 1400°C in vacuum or inert atmosphere to remove the porosity in the matrix. However, partial oxidation of the magnetic component could not be avoided at that high temperature in spite of processing in presence of vacuum or inert atmosphere. Hence, a major

45 problem encountered in many of these magnetic nanocomposites, was the formation of oxide layer over the ferromagnetic core and misleading magnetic properties. Nanocomposites comprising metal nano grains and organic polymers were extensively reported in literature. However, the 50 degradation temperature of polymer based composites is very low and mostly stable only up to 300°C. This restricts their high temperature annealing which is necessary for magnetic ordering [14] of the magnetic component in high density magnetic memory applications.

55 In the present work, fabrication of magnetic nanocomposite with AlPO$_4$ matrix which is almost amorphous is accomplished by synthesizing metal nano particles *in–situ* from inexpensive metal salts following a very simple methodology. The AlPO$_4$ matrix has three distinct advantages: (i) the matrix is almost amorphous 60 and stable up to a very high temperature [15-17], (ii) oxygen diffusivity in the matrix upto very high temperatures is negligible, and (iii) the matrix itself is reducing in nature due to the presence of carbon in smaller percentage (resulted from the burning of organic solvent in air). Hence, metal nano particles 65 could be directly synthesized in air through the reduction of carbon without the addition of foreign reducing agent. It should be noted that addition of highly reactive reducing agents creates the possibilities for undesirable contamination. For example, Ni nano particles synthesized by NaBH$_4$ were usually found to be 70 contaminated by the NiB$_2$ [18]. Although the AlPO$_4$ matrix with embedded graphitized carbon reported for high emissivity applications, still it has never been attempted earlier by any research group for the synthesis of magnetic metal nano particles.
75 The nano-Ni grains in the present study are surrounded by the graphitic carbon envelope which is again distributed in AlPO$_4$ matrix and thus experiencing double protection by the carbon coating and nonmagnetic matrix. The magnetic Ni nano particles

are ferromagnetic at room temperature and showed steadily increasing saturation magnetization with increasing the annealing temperature up to 900°C and are very stable with respect to the oxidation and phase transformation up to this temperature in air. The AlPO$_4$ matrix also preserves its amorphous nature up to 900°C. All the studies including the synthesis of metal nano particles have been performed in air to check the ability of the matrix to protect the metal nano particles synthesized in-situ against oxidation. Therefore, a simple methodology, ease of fabrication avoiding any use of inert atmosphere coupled with the opportunity of using inexpensive precursors and oxidation protection of the magnetic metal nano particles up to a very high temperature in air, offer enormous flexibility for large scale fabrication of the magnetic nanocomposites where magnetic properties of the magnetic component remained largely unaffected.

Experimental

Synthesis procedure-A to obtain black amorphous AlPO$_4$: AlPO$_4$ sol with composition: Al$_{1+x}$PO$_{4+3x/2}$(x=0.75) was prepared from aluminium nitrate and phosphorous pentoxide in ethanolic solution following a technique described elsewhere [15, 16]. An estimated quantity of aluminium nitrate salt was dissolved in ethanol and the solution was mixed with the alcoholic solution of phosphorous pentoxide. The mixed solution was boiled for 15 minutes at ~90°C to get a sol of AlPO$_4$. To synthesize nanocomposites: AlPO$_4$-xNi(x=5, 10), comprising AlPO$_4$ matrix and Ni nano particles, ethanolic solution of estimated quantity of nickel nitrate was mixed with measurable quantity of AlPO$_4$ sol. The sol was dried in oven to get the precursor powders for the composites AlPO$_4$-5 Ni (5 weight % of Ni) and AlPO$_4$-10 Ni (10 weight % of Ni). The oven dried powder was calcined at different temperatures (500° to 1000°C) for 1 hour in air for the crystallization of Ni nano particles in the composites.

Synthesis procedure-B to obtain white amorphous AlPO$_4$: AlPO$_4$ sol with composition: Al$_{1+x}$PO$_{4+3x/2}$(x=0.75) was prepared from aluminium nitrate and di-ammonium hydrogen phosphate as the precursors, and ethylene glycol as the solvent. A required amount of nickel nitrate was added to the precursor gel to obtain the composite: AlPO$_4$ (white) - 5Ni. The dried gel was calcined at 800°C for 1 hour in air.

The X-ray diffraction (XRD) of the powder samples were carried out with a Philips X-ray diffractometer using Cu$_{k\alpha}$ radiation. Thermal stability for the dried gel was carried out using a TG–DTA analyzer (TA Instruments, SDT 2960) between 30 and 1000°C with a heating rate of 10°C /min in air. Carbon analysis of the composite samples were performed using a LECO gas analyzer (model No. CS444, LECO, USA).The particles size and the dispersion of the particles in matrix were investigated with TEM (FEI Tecnai 20T TEM). The samples for TEM observation were prepared by dispersing the powder in ethanol and adding a few drops of the suspension on carbon coated Cu TEM grid. The temperature dependent magnetic properties of the nanocomposite samples were measured with the help of vibrating sample magnetometer (VSM) using magnetic fields upto 2 kOe. The SEM elemental mapping was performed with a Scanning electron microscopy (SEM) (model S4300 HITACHI, Japan) at 20 kV. The oxidation state of the Ni nanoparticles in composites was investigated by X-ray photoelectron spectroscopy (XPS) measurements with a KRATOS AXIS HS spectrometer (using Al KR radiation). The C 1s (binding energy 284.6 eV) peak was considered as a reference line for calibration of the energy scale.

Results and discussion

Calcinations of the oven-dried AlPO$_4$–xNi precursor powder (x=5,10) synthesized following the synthesis procedure–A, mentioned in the experimental section, resulted black powder which was characterized to be a composite of aluminum phosphate (AlPO$_4$), carbon (C) and elemental nickel (Ni) nano particles. In this composite the matrix retained its amorphous nature up to a very high temperature and carbon in the matrix was protected from oxidation due to the extremely low oxygen diffusivity in the mostly amorphous AlPO$_4$ matrix. Concentration of carbon present in the composite calcined at 900^{0}C was determined by the elemental carbon estimation technique and was found to be ~5 weight %. The presence of carbon was also confirmed by Raman spectroscopy which is discussed in the subsequent section of this article. It is to be noted that the alcoholic solvent is the only possible source of carbon present in the composite. Since, no carbonaceous material other than the alcoholic solvent was added with the precursor chemicals.

Thermo gravimetric analysis (TGA) and differential thermal analysis (DTA) measurements were carried out to study the thermal stability and degradation behaviour of the oven-dried precursor powder of the AlPO$_4$-5Ni and AlPO$_4$-10Ni composites (see Fig.1a and b) between 25° and 1000°C in air. The TGA shows weight loss in three steps. The initial weight loss in TGA plot of the gel between 25° and 130°C is associated with the exothermic peak at 85°C (DTA plot) and is attributed to the loss of free moisture. The appearance of a sharp exothermic peak at 173°C in DTA, associated with sharp weight loss between 130° and 170°C in the TGA curve, is due to the ignition of the precursor powder. Above 450°C there is no further weight loss in the TGA and this suggests that the precursor powder burns completely by the ignition reaction. Fig.1b shows the DTA and TGA curves of the as-dried AlPO$_4$-10 Ni precursor powder between 25° and 1000°C in air. The nature of degradation of this composite is similar to that of AlPO$_4$-5Ni.
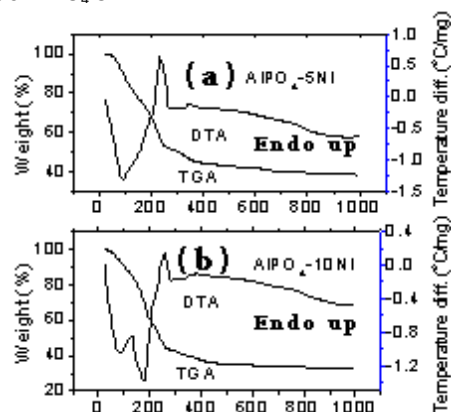

Fig.1. DTA-TGA thermograms for oven dried gels of AlPO$_4$-5Ni and AlPO$_4$-10 Ni composites

Fig.2 shows the XRD patterns of the AlPO$_4$-5 Ni composite calcined at different temperatures (500°-1000°C) in air, showing the crystallization of Ni metal particles in the AlPO$_4$ matrix. The AlPO$_4$ matrix is mostly amorphous in nature which is evident

5 from the broad peak centered at 2θ ~ 22.5^0. It is observed from the XRD diffraction pattern that the peaks for crystalline Ni are absent in AlPO$_4$-5 Ni composite sample calcined at 500°C. It is also obvious that the FCC Ni begins to crystallize at 550°C and is protected from the oxidation up to 900°C in air. However, at

10 1000°C the matrix loses its amorphous nature and is transforming in to the mixture of tridymite and crystobalite AlPO$_4$ phase. The crystallization of AlPO$_4$ is also accompanied by the oxidation of Ni nano particles. It is reported in literature that aluminum phosphate tridymite shows three main characteristic

15 diffraction peaks at 2θ ~20.30^o,21.50^o and 23.02^o (CuK$_\alpha$ radiation) whereas, crystobalite shows an incensed diffraction peak at 2θ ~21.73^o [15-16].
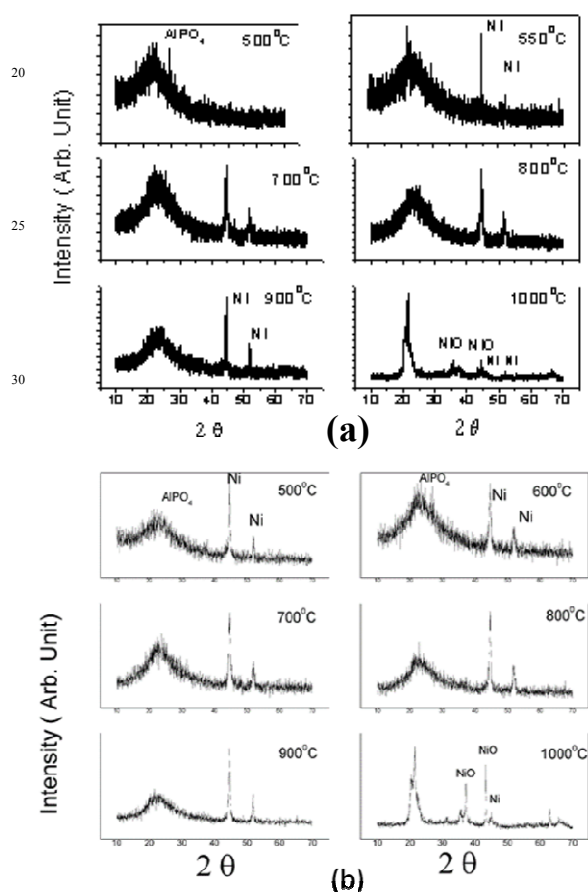

(a)

(b)

Fig.2 XRD of (a) AlPO$_4$-5 Ni and (b) AlPO$_4$-10 Ni nano-composites calcined at different temperatures

35

Additionally, the XRD results revealed three interesting phenomena which occurred during calcination of the dried AlPO$_4$ sol containing nickel nitrate as the precursor for Ni:(i) FCC Ni metal particles crystallize in the matrix instead of forming nickel

40 oxide (NiO) although NiO is expected to be formed upon the calcination of Ni nitrate in air,(ii) Ni metal particles are protected from oxidation up to 900°C in air and (iii) Oxidation of Ni metal particles is accompanied with the sacrificial amorphous nature of the AlPO$_4$ matrix. The nature of the XRD patterns of the AlPO$_4$-10

45 Ni composite calcined at different temperatures (500°-1000°C) in air is similar to that of
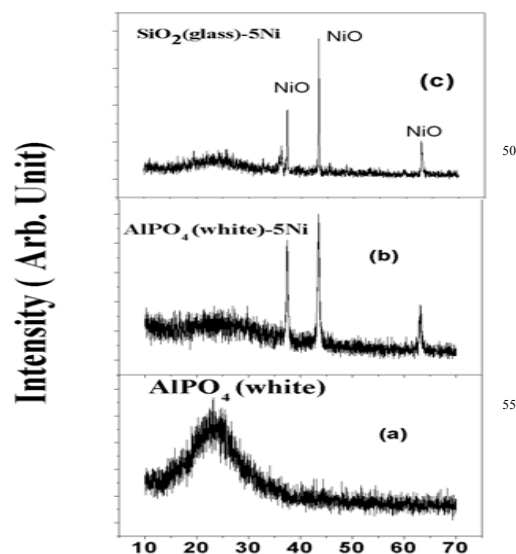
Fig.3. XRD of (a) AlPO$_4$ (white) (b) AlPO$_4$ (white)-5Ni composite
60 calcined at 800°C and (c) SiO$_2$ (glass)-5 Ni composite calcined at 1050°C.

the AlPO$_4$-5 Ni except the crystallization temperature of the former is 500°C whereas for the later is 550°C.It is to be noted
65 that no foreign reducing agents like NaBH$_4$, N$_2$H$_4$ have been introduced during the synthesis of our composites, which are usually observed in the other synthesis techniques to achieve metal nano particles [18, 19]. AlPO$_4$ is not known as a reducing agent and hence the function of AlPO$_4$ in the reduction of NiO to
70 elemental Ni is ruled out. Whereas, the reducing property of carbon is well known and hence the carbon which remains in the matrix in smaller percentage even after calcination of the composite at higher temperatures is believed to be responsible for the reduction of NiO (immediate intermediate product of
75 calcinations of nickel nitrate) to elemental Ni.

In conclusion, the carbon present inside the matrix is responsible for the reduction of NiO to metallic Ni, amorphous white AlPO$_4$ (leaving no carbonaceous residue on calcination) having higher oxygen diffusivity and AlPO$_4$ (white)-5Ni composite
80 were synthesized following the synthesis procedure–B mentioned in the experimental section. The XRD pattern of AlPO$_4$ (white)-5Ni (Fig.3b) calcined at 800°C shows the lines for the NiO signifying that the reduction of NiO to elemental Ni is not possible in this amorphous white AlPO$_4$.

85 It is to be noted that the difference between the white amorphous AlPO$_4$ and black amorphous AlPO$_4$ lies in the difference in oxygen diffusivity. The oxygen diffusivity in white AlPO$_4$ is much higher than that in black AlPO$_4$ which synthesized following the synthesis procedure-A and hence the former
90 procedure cannot protect carbon in air (oxidative atmosphere) while the later can protect the same and appears black in colour after calcination in air. Similar results were observed when SiO$_2$ (glass)-5Ni composite was synthesized using commercially obtained silica paste (the silica paste is known to deliver

amorphous SiO_2 glass on calcinations at higher temperature ($\geq$ 1000°C) (Fig.3c).Therefore, it can be concluded from the XRD characterizations that the immediate product of decomposition of Ni-nitrate in black $AlPO_4$ matrix is NiO and the carbon that is present in the matrix is responsible for instantaneous reduction of the NiO to metallic Ni.
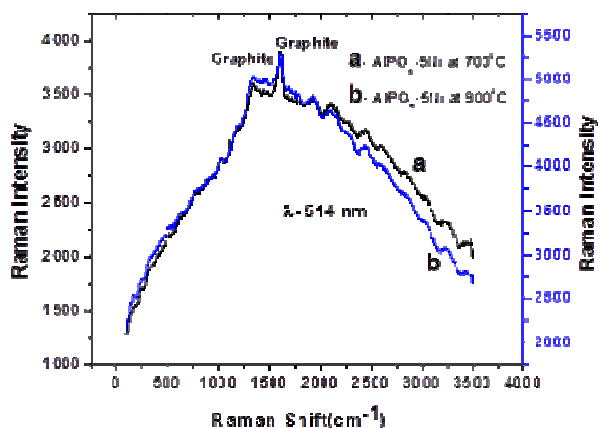

Fig.4. Raman spectra of the $AlPO_4$-5 Ni composite samples calcined at (a) 700° and (b) 900°C
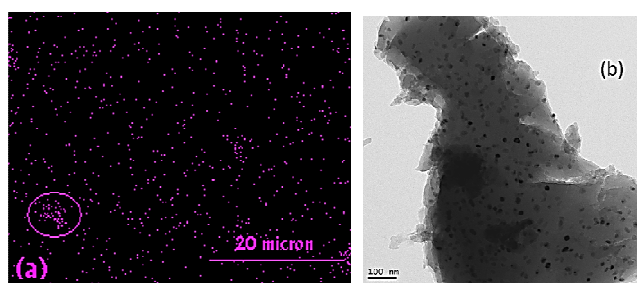

Fig.5. (a) SEM elemental mapping for Ni in composite $AlPO_4$ – 10Ni , portion inside the circle shows the clustering of Ni and (b) TEM micrograph of the700°C calcined composite $AlPO_4$ –5Ni.

Raman spectroscopy was performed on all the $AlPO_4$-x Ni composite samples calcined at 500° - 900°C and it was observed that all the calcined samples showed peaks for carbon in Raman spectra. Fig. 4a and b show the Raman spectra of the $AlPO_4$-5 Ni composite samples calcined at 700° and 900°C, respectively. The peaks at 1345 cm^{-1} and 1600cm^{-1} can be attributed to the presence of D-band and graphitic carbon G-band as reported earlier in literature by Wang *et.al.*[20] and Tuinstra *et.al.* [21].

No further study was performed on white amorphous $AlPO_4$ since elemental Ni was not obtained in this matrix and attention was paid to explore the composites of black amorphous $AlPO_4$ and elemental Ni($AlPO_4$–xNi) , which were obtained following the synthesis procedure –A. In order to understand how the elemental Ni nano particles are distributed in $AlPO_4$ matrix the SEM elemental mapping was performed and the result is shown in Fig. 5a. It is observed that the Ni is evenly distributed in the matrix except in some portions it is forming clusters and it was confirmed from the elemental mapping and microstructure of the clusters that even in the cluster, the $AlPO_4$ coated Ni nano

particles do not adhere together to form larger aggregates although coming close proximity to each other. Fig. 5b shows TEM micrograph of the $AlPO_4$–5Ni composite calcined at 700°C. The average size of the Ni nano particles varies from 10 nm to 15 nm. TEM studies of the nano particles in higher magnification revealed that most of the particles are covered by graphitized carbon and this carbon envelope is intact even in the composite samples calcined at 900°C (Fig.6a-d).
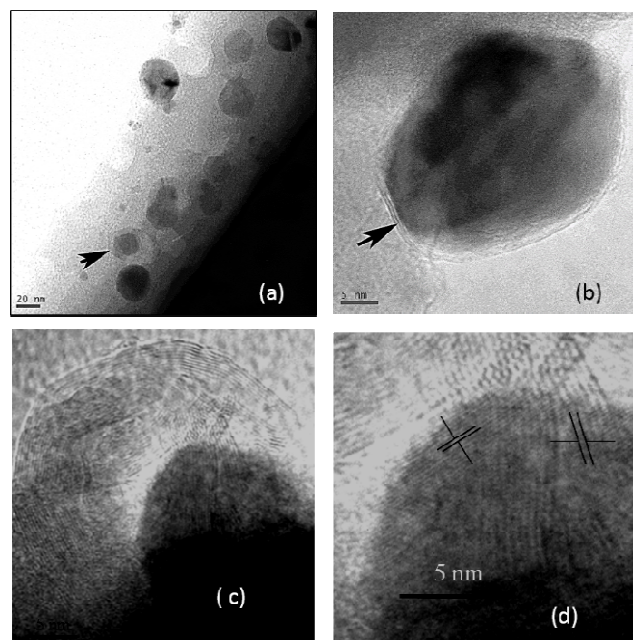

Fig.6(a)TEM micrograph of the 900°C calcined composite $AlPO_4$ – 10Ni (b) the same at higher magnification (the arrows in Fig. 6a and b indicate the graphitized carbon coating at the periphery of the Ni particles)(c)Ni nano particle in the same composite with hexagonal graphitized carbon envelope and (d) Enlarged portion 'A' showing the crystal planes of elemental Ni(d=2.03Å)(111 plane) and graphitized carbon(d=3.30Å)(002 plane).

X-ray photoelectron spectroscopy (XPS) was performed on the nanocomposite samples to analyze the presence of any NiO layer on the surface of the Ni nano particles. XPS analyses indicate the presence of minor amounts of NiO (satellite peaks at 879.9 and 861.9 eV) along with Ni (0) (Ni 2p $^{3/2}$ and Ni 2p$^{1/2}$ peaks at 856 and 873.9 eV) as shown in Fig.7. However, it is believed that majority of the Ni nano particles which are buried deep inside the oxidation resistant $AlPO_4$ matrix must not contain any NiO layer. The Ni nano particles which are situated at the surface of the composites are partially dipped in the matrix and are unprotected as shown in TEM micrograph in Fig.8. These surface nano particles develop NiO layer surrounding themselves on calcinations at higher temperatures in air. This conclusion has been drawn based on the following facts:

(i) The depth of the X-ray penetration in XPS is limited to 50Å beyond the surface only, means it can analyze only the surface Ni nano particles which are unprotected and are oxidized.
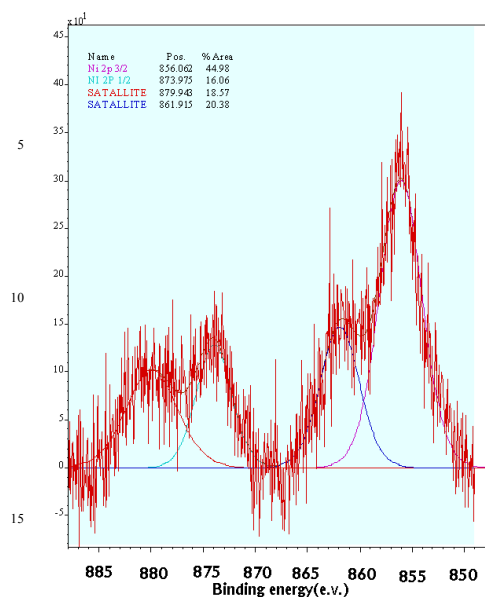
Fig.7. XPS spectra of the $AlPO_4$ –10Ni composite sample calcined at 900^{0}C showing the Ni 2p $^{3/2}$ and Ni 2p$^{1/2}$ peaks at 856 and 873.9 eV respectively and satellite peaks at 879.9 and 861.9 eV respectively for NiO.
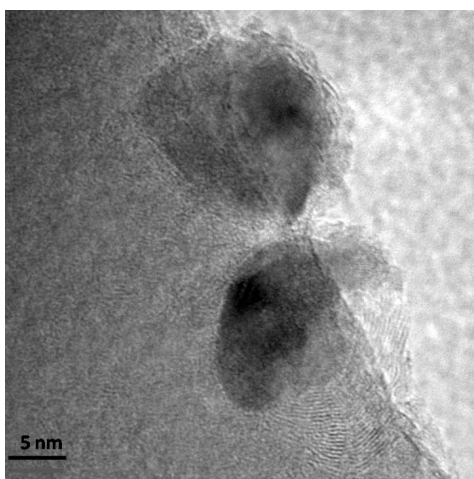

Fig. 8.TEM micrograph of unprotected Ni nano particles partially dipped in the $AlPO_4$ matrix in 900^{0}C calcined $AlPO_4$–10Ni composite

Hence, detection of the Ni nano particles beyond this depth inside the matrix is not possible by XPS.

(ii) If the Ni nano particles which are protected inside the $AlPO_4$ matrix   would undergo surface oxidation then overall magnetization value would decrease with increasing the calcination temperature since for all the samples calcinations were performed in air and thickness of the NiO layer surrounding the Ni nano particles are expected to increase with increasing calcinations temperature. It must be noted that the NiO is not magnetic and presence of NiO layer must decrease the magnetization value for the composite samples calcined at higher temperatures. Table 1 shows just the opposite phenomena i.e. the magnetization values are increasing with increasing calcinations temperature up to 900^{0}C.

Magnetic properties were characterized by vibrating sample magnetometer (VSM) and magnetization versus applied magnetic field (M-H) curves were recorded at room temperature (300 K) for both the composite samples as shown in Fig.9 and Fig.10. The hysteresis curves are typically of ferromagnetism in nature and the saturation magnetization (Ms) increased with increasing the calcinations temperature for both the composite samples. Moreover, the value of Ms for $AlPO_4$ –10Ni at each calcination temperature is almost doubled of that for $AlPO_4$ –5Ni (table1).Very low value of magnetization for the $AlPO_4$– 5Ni composite calcined at 500^{0}C is concurrent with the XRD result of the same which shows lack of crystallinity of Ni nano particles in this composite at 500^{0}C (Fig.2a), whereas Ni nano particles in the nano composite $AlPO_4$–10Ni are crystalline when calcined at that temperature, as indicated in Fig.2b. Ms is marginally higher for $AlPO_4$–10Ni composite calcined at 500^{0}C than that of the sample calcined at 500^{0}C which contradicting the statement made that Ms is increasing with increasing the calcination temperature. However, this slight decrease in magnetization between 500^{0}C and 550^{0}C may not be regarded as the usual trend since Ms increases steadily with increasing the calcination temperature from 550^{0}C to 900^{0}C. Overall, there is an increasing trend if the slight variation between the samples calcined at 500^{0}C and 550^0 C is ignored.
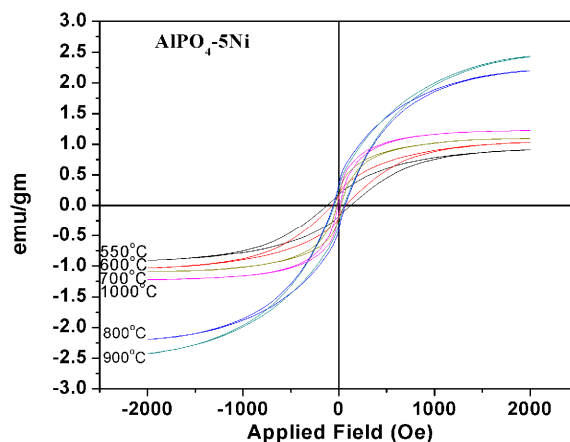

Fig.9. Magnetization versus field curve measured at room temperature for $AlPO_4$ –5Ni calcined at different temperatures in air.

It is known that presence of any interstitial atoms like carbon (C), oxygen (O) will decrease the magnetic moment of Ni atom. The lower magnetization value of 500^{0}C sample is attributed to the presence of residual C in the Ni particles as the C acts as reducing agent of NiO during calcinations. When calcinations temperature is increased from 500–900^{0}C, the dissolved residual C diffuse to the surface of Ni particle and forms carbon layer around the Ni nano particle which is evident from the high resolution TEM image. High resolution TEM of 700^{0}C calcined $AlPO_4$–10Ni shows hexagonal carbon is dissolved in Ni nano particles resulting hexagonal shaped Ni nano particles, however, carbon layers at the periphery of the Ni nano particles are not detected as it is observed for 900^{0}C calcined $AlPO_4$–10Ni. Hence, it is believed that diffusion of carbon from Ni particle-core to the surface led to the increase in magnetization with increasing
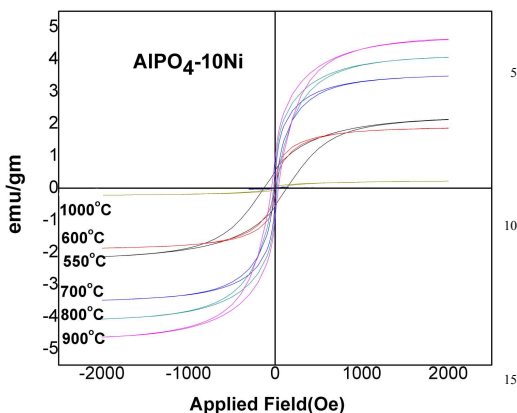
calcinations temperature.

Fig.10. Magnetization versus field curve at room temperature for AlPO$_4$ –10Ni calcined at different temperatures in air.

Table 1. Magnetization Values for AlPO$_4$ –5Ni and AlPO$_4$ –10Ni calcined at different temperatures

Calcination Temp.	Composite: AlPO$_4$ –5Ni			Composite: AlPO$_4$ –10Ni		
	M$_s$ of the composite emu/gm	M$_s$ of Ni emu/gm	μ$_B$* per Atom	M$_s$ of the composite emu/gm	M$_s$ of Ni emu/gm	μ$_B$ per Atom
500°C	0.1	2.1	0.02	2.5	24.8	0.26
550°C	0.9	18.2	0.20	2.1	21.3	0.20
600°C	1.0	20.8	0.23	2.3	22.7	0.24
700°C	1.8	36.7	0.38	3.5	34.9	0.37
800°C	2.2	44.1	0.46	4.1	40.7	0.43
900°C	2.4	48.7	0.51	4.6	46.4	0.49
1000°C	1.2	24.5	0.25	0.2	2.2	0.02

*'μ$_B$' is magnetic moment

Maximum M$_s$ of nano Ni distributed in both AlPO$_4$–5Ni and AlPO$_4$–10Ni calcined at 900°C are measured to be 48.7 emu/gm and 46.4emu/gm, respectively. The respective 'bulk' value for fcc Ni is 55 emu/g at room temperature. Hence, it can be concluded that the magnetization of Ni in the composites approached to maximum of 89% of the corresponding bulk magnetization value. The lower saturation magnetization values for nano Ni are reported earlier in the literature and is believed to be caused by the surface defects, oxygen contamination etc. [19, 22]. Above 900°C the magnetization decreases abruptly due to the oxidation of the Ni particles. The results of this study might be exploited for high density magnetic recording media applications. e.g. HAMR (Heat Assisted Magnetic Recording), where it magnetically records data on high-stability media using laser thermal assistance to first heat the material. HAMR takes advantage of high-stability magnetic compounds, which is achieved by heating the materials before applying the changes in magnetic orientation [23-24].

Conclusions

Ni nano particles could be generated in the nearly amorphous AlPO$_4$ matrix without using any foreign reducing agent. The carbon which routed from the burning of the solvent during calcination was responsible for the in situ reduction of NiO to elemental Ni in the AlPO$_4$ –xNi composites. Ni nano particles were protected from oxidation in the amorphous AlPO$_4$ matrix up to 900°C. Oxidation of Ni nano particles above 900°C was accompanied with the increase in crystallinity of the matrix. Ni nano particles in the AlPO$_4$ matrix were coated by graphitized carbon which remained intact even when the composite was calcined at 900°C. The sizes of the individual carbon coated Ni particles varied from 10 to 15 nm. Magnetization in both the AlPO$_4$–5Ni and AlPO$_4$–10Ni composites increased with increasing the calcination temperature up to 900°C. Above 900°C the magnetization decreased abruptly due to oxidation of the Ni particles. Magnetization of Ni in the composites was proportional to the amounts of Ni particles in the composites. The results of this experiment were very promising as that created important possibility of studying magnetic metal/alloy nano particles up to 900°C in oxidative atmosphere without oxidation of the metal/alloy nano particles which might be exploited for high density magnetic recording media applications.

Notes and references

*a*Defence Metallurgical Research Laboratory, Hyderabad -500058, A.P., India.Fax: 040-24340863; E-mail: r_subir@dmrl.drdo.in; r_subir@yahoo.com
*b*School of Engineering Sciences and Technology, University of Hyderabad, Gachibowli, Hyderabad 500 046, A.P. India, ; Tel: 04023134457; Fax: 040-23011089, E-mail: ppse@uohyd.ernet.in, pradip.paik@gmail.com

† Electronic Supplementary Information (ESI) available: [details of any supplementary information available should be included here]. See DOI: 10.1039/b000000x/

‡ Footnotes should appear here. These might include comments relevant to but not central to the matter under discussion, limited experimental and spectral data, and crystallographic data.

1 J.A. Bas, J.A. Calero and M.J. Dougan, *J. Magn. Magn. Mater.,*2003,**391**, 254/255.

2 H.Y. Jiang , W. Zhonga, X.L. Wu , N.J. Tang , W. Liu and Y.W. Du,*Journal of Alloys and Compounds* 2004,**384**, 264–267.

3 D.Kumar, H.Zhou, T.K Nath, A.V.Kvit and Narayan, J. *Appl. Phys. Lett.,*2001**, 79**, 2817.

4 D.N.Lambeth, E.M.T. Velu, G.H.Bellesis, L.L.Lee and D.E. Laughlin, *J. Appl. Phys*., 1996, *79*, 4496.

5 S.Sun, C.B. Murray, D. Weller, L.Folks and A. Moser, *Science,* 2000**, 287**, 1989.

6 U.Hofeli, W.Schutt, J.Teller and M. Zborowski, *In Applications of Magnetic Carriers,* (Plenum), New York, 1997.

7 A.J.Van Dillen,R.J. Ter ¨ orde, D.J. Lensveld, J.W.Geus and K.P. Jong, *J. Catal*., 2003, **216**, 257.

8 S.Takahashi and S. Maekawa, *Phys. Rev. Lett.,* 1998, **80**, 1758.

9 A. Gavrin and C. L. Chen, *J. Appl. Phys*.**,** 1993,**73**, 6949

10 E. M. Gonza´lez, M. I. Montero, F. Cebollada, C. de Julia´n, J. L.Vicent, and J. M. Gonza´lez, *Europhys. Lett.*, 1998, **42**, 91.

11 J. S. Jung, W. S. Chae, R. A. McIntyre, C. T. Seip, J. B. Wiley, and C. J. O'Connor, *Mater. Res. Bull.,*1999, **34**, 1353.

12 C. Estourne`s, T. Lutz, J. Happich, T. Quaranta, P. Wissler, and J. L. Guille, *J. Magn. Magn. Mater.,*1997,**173**, 83.

13 E. R. Leite, N. L. V. Carren˜o, E. Longo, A. Valentini, and L. F. D. Probst, *J. Nanosci. Nanotechnol.,*2002,**2**, 89.

14 H. Hatafuku and S. Takahashi, *IEEE Trans. Magn.,*1996, **32**, 1959.

15 S.Sambasivan ,*U.S. Patent No.*: 6,036,762 (**2000).**

16 S.Sambasivan, and K.A.Steiner, *U.S. Patent No.*: 6,461,415 **(2002).**

17 F. Guti´errez-Mora , K.C. Goretta , D. Singh,, J.L. Routbort , S. Sambasivan , K.A. Steiner , J. Adabie and K.K. Rangan, *J. Euro. Ceram. Soc.,*2006, **26**, 1179–1183.

18 Elisabeta Mitran, Barry Dellinger, and Robin L. McCarley*, Chem. Mater*. 2010, **22**, 6555–6563.

19 Aparna Roy , V. Srinivas, J. A. De Toro and U. Mizutani, *Phys. Rev.,*2005**,** B **71**, 184443.

20 Yan Wang, C.Daniel, Alsmeyer and Richard L. Mc Creery, *Chem. Mater*., 1990, **2**, 557-563.

21 F. Tuinstra and J.L. Koenig, Journal of Chemical Physics, 1970, **V-53**(3).

22 Jai Prakash, A. Tripathi, J.C. Pivin, Jalaj Tripathi, A.K. Chawla, Ramesh Chandra, S.S. Kim, K. Asokan and D.K. Avasthi,*Adv. Mat. Lett*.**,** 2011,**2(1),** 71-75.

23 S.N.Piramanagam,,J.Z.Shi,H.BZaho,C.K.Pol,C.S.Mah,C.Y.Ong,J.M.Zhao,J.Zhang,Y.S.Kay and L.Lu.IEEE Trans.magn. 2007, **43**, 633.

24 C.P.Luo,S.H.Liuo,L.Gao,YLiu and D.J.Sellmyer, J. Appl. Phys.Lett. 2000, **77**, 2225.

Fig.1. DTA-TGA thermograms for oven dried gels of $AlPO_4$-5Ni and $AlPO_4$-10 Ni composites.

5

Fig.2 XRD of (a) $AlPO_4$-5 Ni and (b) $AlPO_4$-10 Ni nano-composites calcined at different temperatures.

Fig.3. XRD of (a) $AlPO_4$ (white) (b)$AlPO_4$ (white)-5Ni composite calcined at 800^0C and (c)SiO_2(glass)-5 Ni composite calcined at 10 1050^0C.

Fig.4. Raman spectra of the $AlPO_4$-5 Ni composite samples calcined at (a) 700° and (b) 900^oC .

Fig. 5. (a)SEM elemental mapping for Ni in composite $AlPO_4$ – 15 10Ni , portion inside the circle shows the clustering of Ni and (b) TEM micrograph of the700^oC calcined composite $AlPO_4$ –5Ni.

Fig.6(a)TEM micrograph of the 900^oC calcined composite $AlPO_4$ – 10Ni (b) the same at higher magnification (the arrows in Fig. 6a and b indicate the graphitized carbon coating at the periphery of 20 the Ni particles)(c)Ni nanoparticle in the same composite with hexagonal graphitized carbon envelope and (d)Enlarged portion 'A' showing the crystal planes of elemental Ni(d=2.03Å)(111 plane) and graphitized carbon(d=3.30Å)(002 plane).

25 Fig.7. XPS spectra of the $AlPO_4$ –10Ni composite sample calcined at 900^0C showing the Ni 2p $^{3/2}$ and Ni 2p$^{1/2}$ peaks at 856 and 873.9 eV respectively and satellite peaks at 879.9 and 861.9 eV respectively for NiO.

8.TEM micrograph of unprotected Ni nanoparticles partially 30 dipped in the $AlPO_4$ matrix in 900^0C calcined $AlPO_4$ –10Ni composite.

Fig.9. Magnetization versus field curve measured at room temperature for $AlPO_4$ –5Ni calcined at different temperatures in air.
35 Fig.10. Magnetization versus field curve at room temperature for $AlPO_4$ –10Ni calcined at different temperatures in air.

40

45